Supporting Information

Spherical and Fibril-Shaped Nanoparticles as Shape-Dependent MRI Contrast Agents

Lyndsay M. Randolph,[%,‡] Clare L. M. LeGuyader,[%,‡] Michael E. Hahn,[%,&,‡,] Christopher M. Andolina,[$] Joseph P. Patterson,[%] Robert F. Mattrey,[&] Jill E. Millstone,[$] Mauro Botta,[@] Miriam Scadeng,[&] and Nathan C. Gianneschi,[%*]*

[%]Department of Chemistry and Biochemistry, University of California, San Diego, 9500 Gilman Dr., La Jolla, CA 92093, United States, [&]Department of Radiology, University of California, San Diego, 9500 Gilman Dr., La Jolla, CA 92093, United States, [$]Department of Chemistry, University of Pittsburgh, 4200 Fifth Ave, Pittsburgh, PA 15260, United States, [@]Dipartimento di Scienze e Innovazione Tecnologica, Università del Piemonte Orientale "A. Avogadro", Alessandria, Italy. [‡]These authors contributed equally.

Experimental methods

Monomer and Polymer Synthesis and Characterization

All reagents were purchased from Sigma-Aldrich or Macrocyclics and used without further purification. RP-HPLC analyses were performed on a Jupiter 4μ Proteo 90Å Phenomenex column (150 x 4.60 mm) with a binary gradient at a flow rate of 1 mL/min using a Hitachi-Elite LaChrom L-2130 pump equipped with UV-Vis detector (Hitachi- Elite LaChrom L-2420). For purification, a semi-preparative Phenomenex Jupiter 4μ Proteo 90Å column (250 x 10.0mm) was utilized at a flow rate of 4 mL/min. For both analytical and semi-preparative RP-HPLC, the following mobile phases were used: Eluant A = 0.1% TFA in water; Eluant B = 99.9% acetonitrile, 0.1% TFA. ^{1}H (300 and 400 MHz) and ^{13}C (100 MHz) NMR spectra were recorded on a Varian Mercury Plus spectrometer. Mass spectra were obtained at the UCSD Chemistry and Biochemistry Molecular Mass Spectrometry Facility. Polymer

dispersities and molecular weights were determined by size-exclusion chromatography (Phenomenex Phenogel 5μ 10E3A, 1K-75K, 300 x 7.80 mm in series with a Phenomex Phenogel 5μ 10E3A, 10K-1000K, 300 x 7.80 mm (0.05 M LiBr in DMF or HPLC grade $CHCl_3$) using a Shimatzu pump equipped with a multi-angle light scattering detector (DAWN-HELIOS: Wyatt Technology) and a refractive index detector (Hitachi L-2490) normalized to a 30,000 MW polystyrene standard using dn/dc of 0.179.

Gadolinium concentration determination

Standard Curve for Gd^{3+} Concentration Determination. A 0.1 M stock solution of $GdCl_3$ in H_2O was prepared. From this stock, concentrations of 3.0, 1.0, 0.5, and 0.01 mM of Gd^{3+} in 2:3:5 HNO_3:H_2O:D_2O were made. T_1 relaxations were determined for each concentration of Gd^{3+} using inversion recovery experiments on a 300 MHz Varian NMR instrument. $1/T_1$ were averaged for three separate samples at the same concentration, then plotted to give a relaxivity of free Gd^{3+} of 13.8 $mM^{-1}sec^{-1}$ ± 0.830 with an R^2 value of 0.9992.

General Procedure to Determine Concentration of Gd^{3+} for SMN and FMN. In order to determine Gd^{3+} concentration, the metal was first stripped from the chelate using concentrated nitric acid. 80% HNO_3 in water (115 μL) was added to an aliquot of each sample (115 μL). Each mixture was then heated at 65 ºC for approximately 12 hours. The sample was diluted with 230 μL of D_2O and T_1 was determined using an inversion recovery experiment on a 300 MHz Varian NMR. Based the standard curve created above, the concentration of Gd^{3+} in stock solutions of SMN and FMN were determined to be 0.408mM and 0.444mM, respectively.

^{1}H NMRD Instrmental Set-up and Profiles

Proton $1/T_1$ NMRD profiles were measured on a Fast Field-Cycling Stelar SMARTracer NMR Relaxometer (Stelar, Mede (PV), Italy) over a continuum of magnetic field strengths from 0.00024 to 0.25 T (corresponding to 0.01-10 MHz proton Larmor frequencies). The

relaxometer operates under computer control with an absolute uncertainty in $1/T_1$ of ± 1%. Additional data points in the range 20-70 and 400 MHz were obtained on a Bruker WP80 NMR electromagnet adapted to variable-field measurements (15-80 MHz proton Larmor frequency) Stelar Relaxometer and Jeol ECP spectrometer (9.39 T), respectively. The ^1H T_1 relaxation times were acquired by the standard inversion recovery method with typical 90° pulse width of 3.5 μs, 16 experiments of 4 scans. The temperature was controlled with a Stelar VTC-91 airflow heater equipped with a calibrated copper–constantan thermocouple (uncertainty of ±0.1 °C). The temperature was determined by previous calibration with a Pt resistance temperature probe.

In Vitro and In Vivo MRI

MR images were acquired on a Bruker 7.0 T magnet with Avance II hardware equipped with a 72 mm quadrature transmit/receive coil. Axial MR images were acquired using a standard T_1-weighted sequence with a repetition time of 3249.2 ms, time to echo of 7.6 ms, with fat suppression, a matrix of 256 x 256, field of view (FOV) of 4.00 x 3.00 cm, resolution of 156 x 117 microns, slice thickness of 1.00 mm, inter-slice distance of 1.00 mm, 80 slices. T_1 shortening was determined by selecting regions of interest (ROI) using Software ParaVision Version 5.1 from T_1-T_2 map with the following parameters: Times to echo of 11, 33, 55, 77, and 99 ms and 6 repetition times of 5000, 3000, 2500, 2000, 1500, and 1200 ms, and a flip angle of 180º.

Analysis of T_1 Data

To correct for minor scan-to-scan variations due to noise, T_1 was normalized to pre-injection phantom relaxivities. Phantoms of Gd-DOTA, SMN or FMN, were included in each scan corresponding to the material injected. Concentrations selected were 0.41, 0.12, 0.033, 0.0095, and 0.0027 mM with respect to Gd^{3+} in H_2O. Pre-injection relaxivities were generated for each mouse by averaging $1/T_1$ (r_1) values (sec^{-1}) for each phantom concentration over

selected slices of the mouse (The selected slices were those in which the organs of interest were visible). For each scanning time point after injection, an average $1/T_1$ for 5 phantoms were calculated and compared to the pre-injection relaxivity value to generate an adjustment factor for the scan of interest. Relaxivity values generated from phantoms for each scan were within (+/-) 1 - 20% of the pre-injection phantom relaxivity. After organ ROI T_1 was converted to $1/T_1$, each were multiplied by the adjustment factor. $1/T_1$ was averaged over each organ and then converted back to T_1 (msec). Normalized T_1 were averaged over three mice for each time point sampled and each material. Error for urinary bladder and liver are standard errors, over three mice for each material, using normalized T_1 for each specific time point sampled.

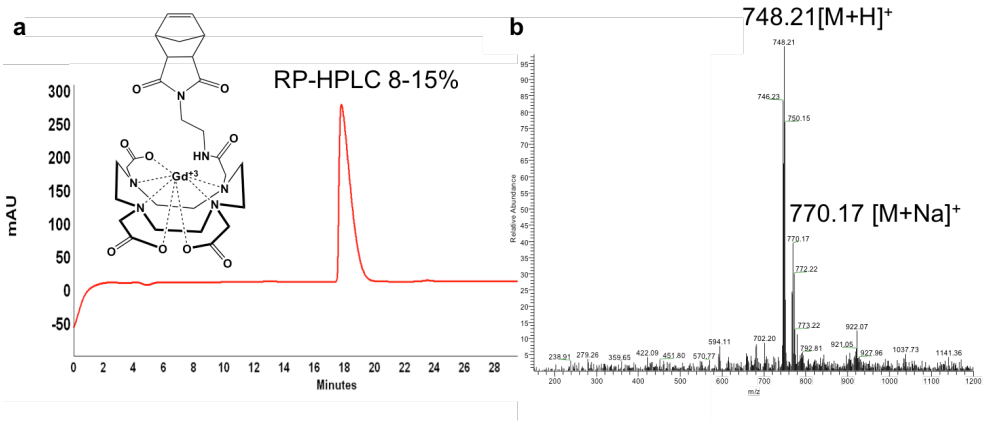

Figure S1. Monomer 2 characterization following purification by RP-HPLC.

a) *Analytical RP-HPLC chromatogram of purified monomer* ***2***

b) *LR-ESI-MS: found m/z 748.21, expected m/z 748.19 M+H$^+$; found m/z 770.17, expected m/z 770.18 M+Na$^+$*

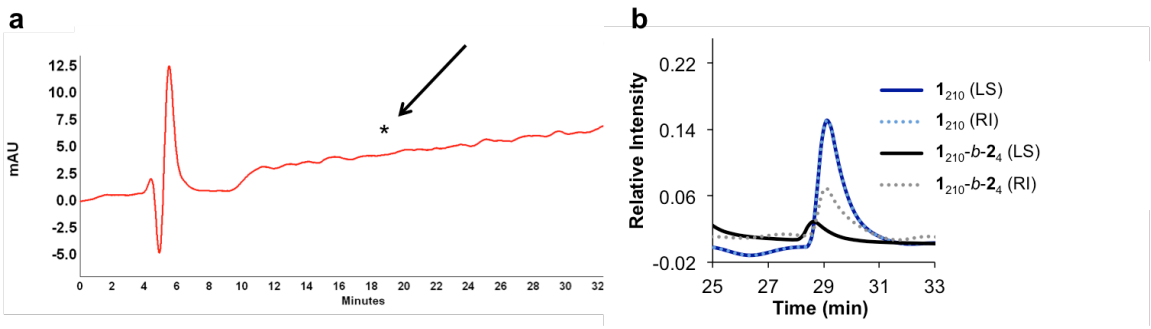

Figure S2. Characterization of 1_{210}-*b*-2_4.

a) *Analytical RP-HPLC chromatogram of reaction mixture demonstrating consumption of monomer **2**. Expected retention time of monomer **2** is highlighted with an asterisk.*

b) *SEC-MALS and RI analyses of homopolymer **1** and block copolymer **1**-b-**2** in $CHCl_3$: Homopolymer **1**: Mn = 53,150, Mw/Mn = 1.027, DP = 210. Copolymer of **1**-b-**2**: Mn = 55,740, Mw/Mn = 1.004, DP = 4.*

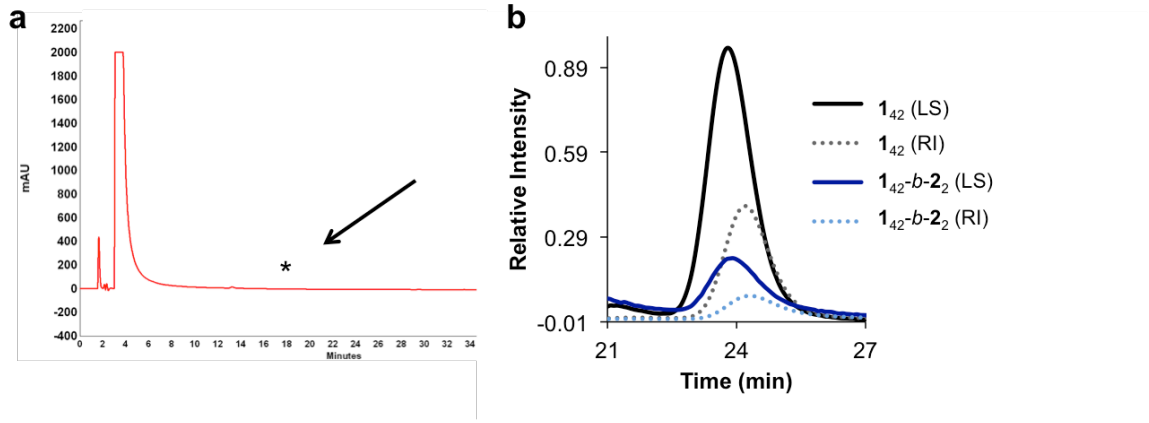

Figure S3. Characterization of 1_{42}-*b*-2_2.

a) *Analytical RP-HPLC chromatogram of the reaction mixture demonstrating consumption of monomer **2**. Expected retention time of monomer **2** is highlighted with an asterisk.*

b) *SEC-MALS and RI analyses of homopolymer **1** and block copolymer **1**-b-**2** in 0.05 M LiBr in DMF: Homopolymer **1**: Mn = 10,560, Mw/Mn = 1.013, DP = 42. Copolymer **1**-b-**2**: Mn = 11,910, Mw/Mn = 1.024, DP = 2.*

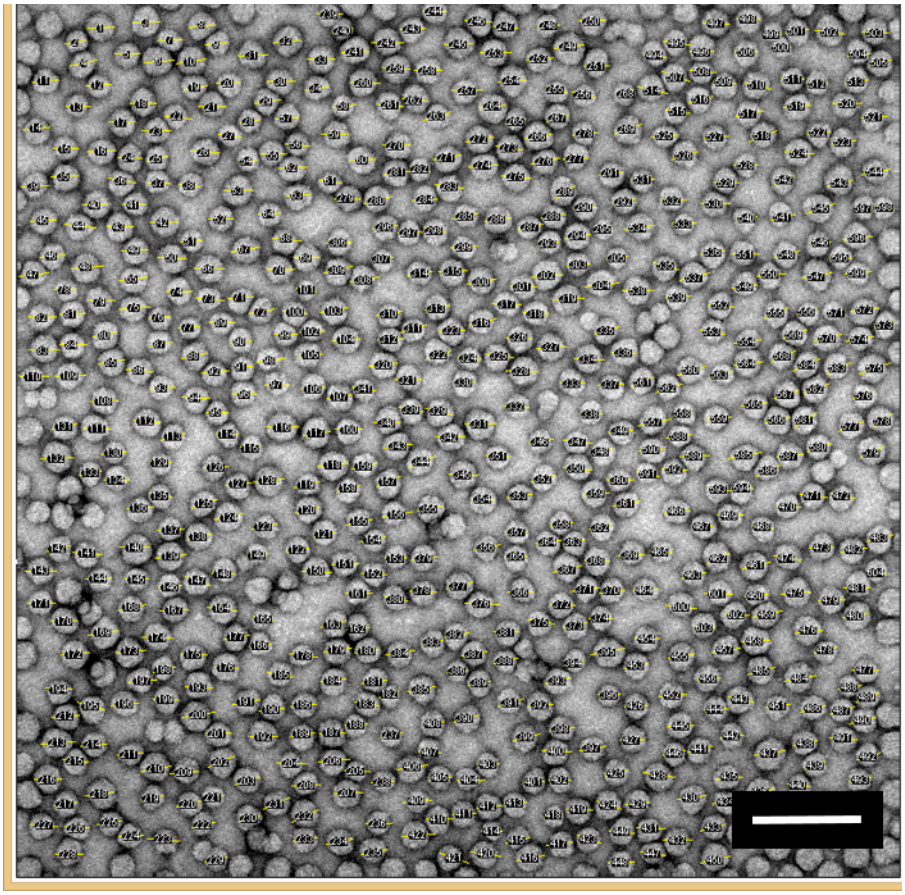

Figure S4. SMN phase analysis. TEM image analyzed for sphere diameter uniformity (scale bar = 100nm). Diameters of particles were measured in ImageJ, as indicated by the yellow lines in the above representative TEM image. 604 particles were counted, and found to have an average diameter of 24.7 nm, with a standard deviation of 2.9 nm.

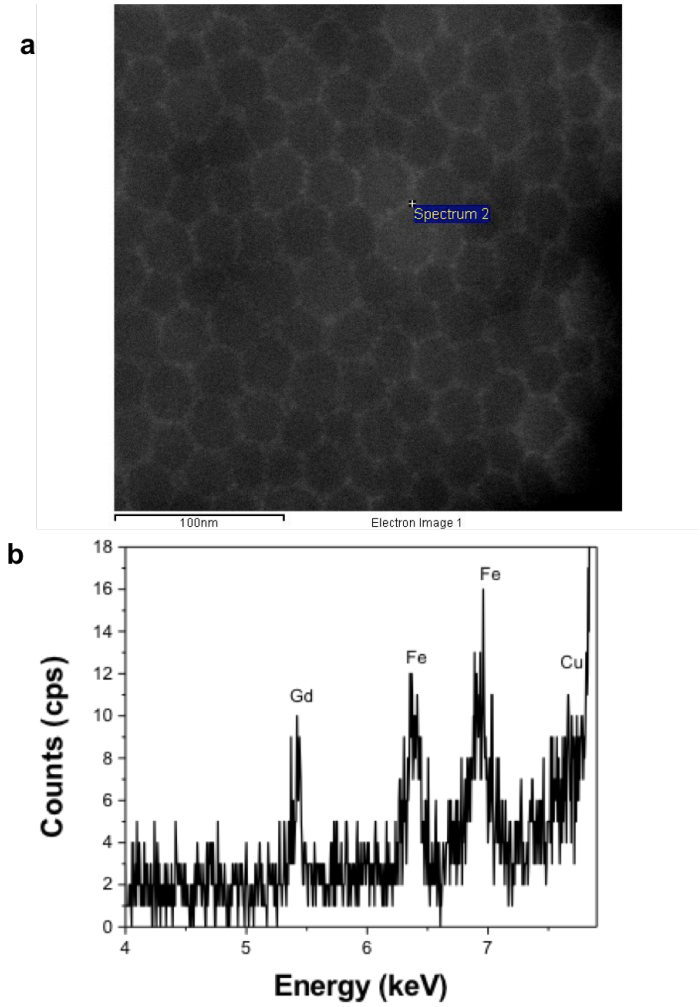

Figure S5. STEM-EDS Analysis of SMN.

a) *STEM-HAADF of SMN with area chosen for EDS analysis (annotated as spectrum 2).*

b) *EDS of SMN from the area selected in (a). Iron and copper signals are artifacts from the specimen holder and copper grid.*

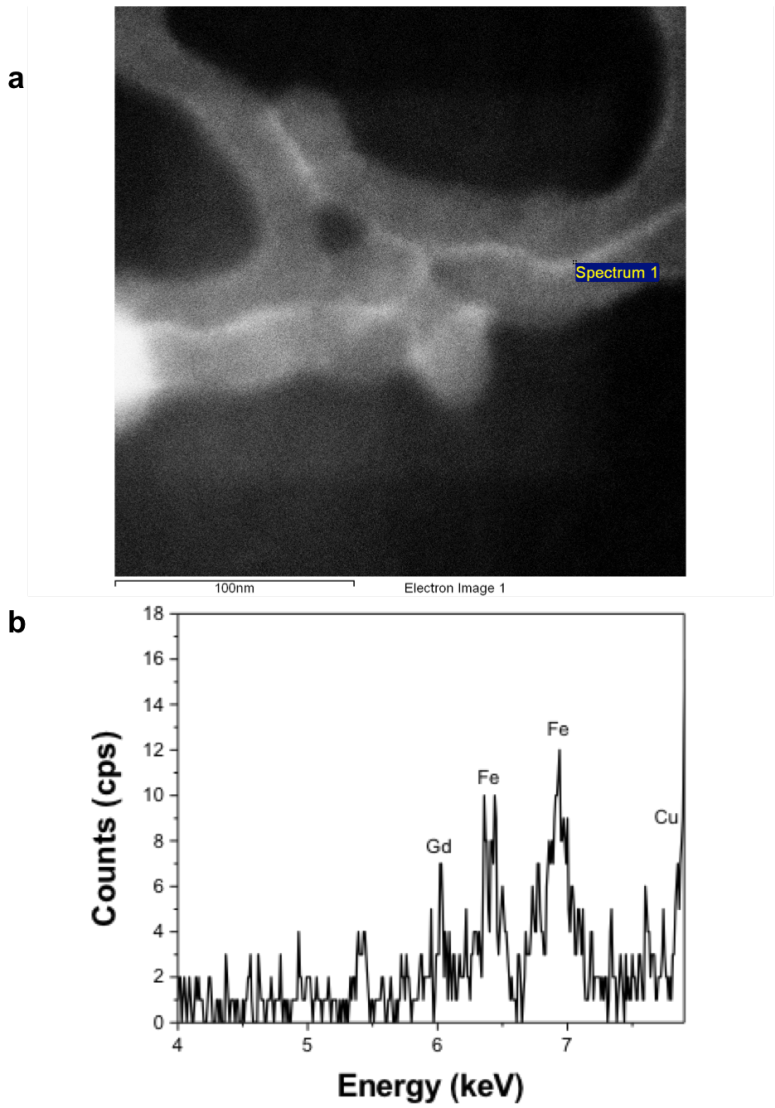

Figure S6. STEM-EDS Analysis of FMN.

a) *STEM-HAADF of FMN with area chosen for EDS analysis (annotated as spectrum 1).*

b) *EDS of FMN from the area selected. Iron and copper signals are artifacts from the specimen holder and copper grid.*

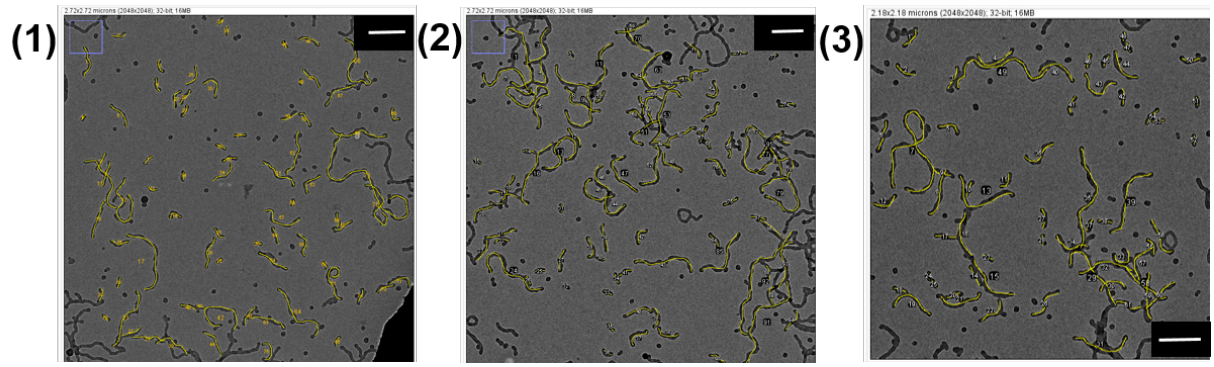

Figure S7. FMN phase analysis. Three TEM images were analyzed for %volume fibrillar phase (scale bar = 250nm). Lengths of fibrillar particles were measured in ImageJ, as indicated by the yellow lines above in representative TEM images (1)-(3), above. Diameter of the fibers was assumed to be the same as the spheres, and volume was calculated using the average sphere radius. Volume of the spheres was calculated accordingly, and summation of volume of tabulated spheres and fibers was used to determine respective ratios, as listed in Table S1.

Table S1. Measured volumes of spheres and non-spheres in FMN.

image#	total measured volume (nm^3)	fraction non-sphere	%non-sphere	
1	0.013	0.941	94.1	
2	0.021	0.963	96.3	
3	0.011	0.948	94.8	
	average % volume non-sphere		95.1	

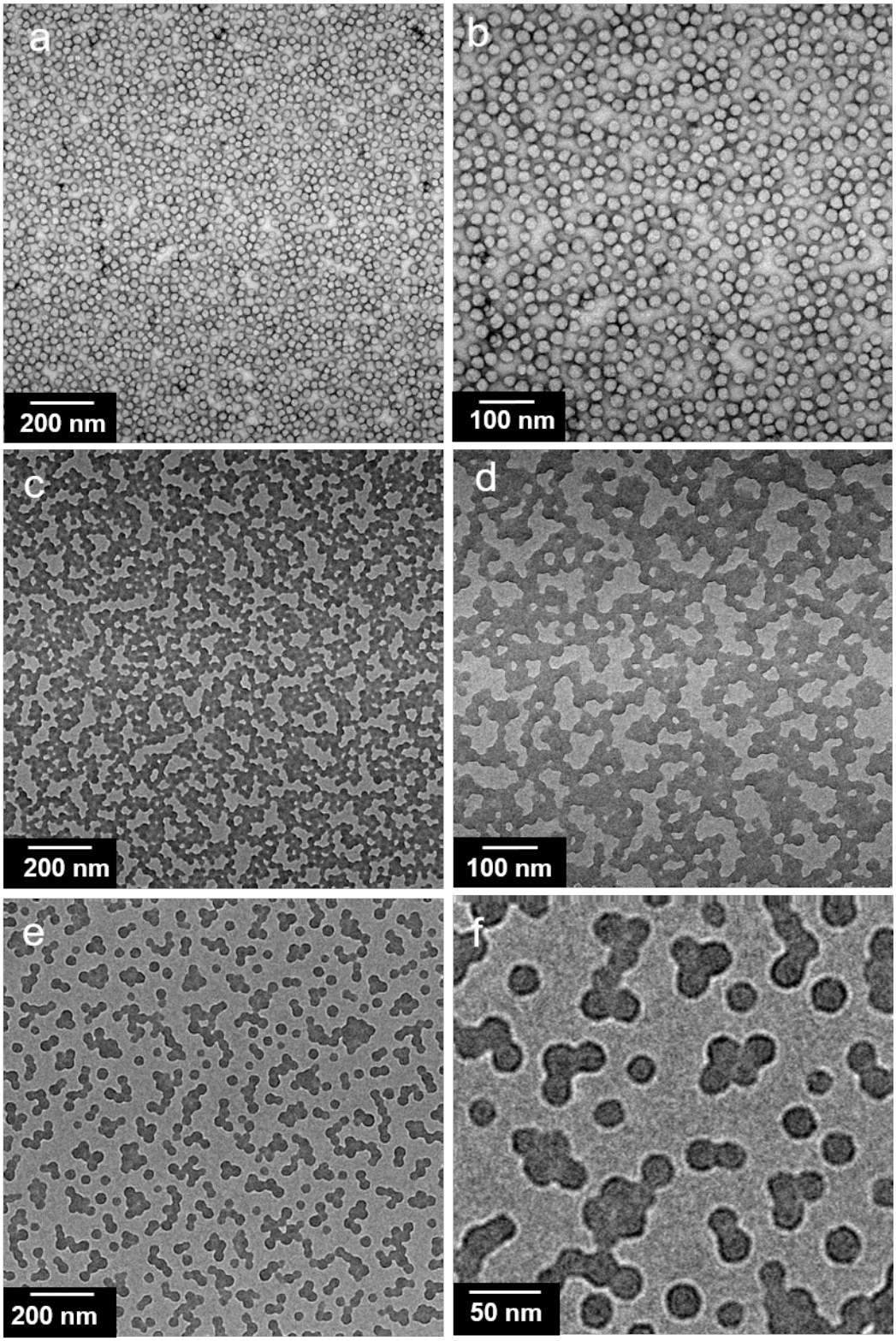

Figure S8. TEM of SMN, imaged 14 months after preparation.

a) and b) TEM of SMN, negative staining using 1% uranyl acetate

c)-f) TEM of SMN, no staining

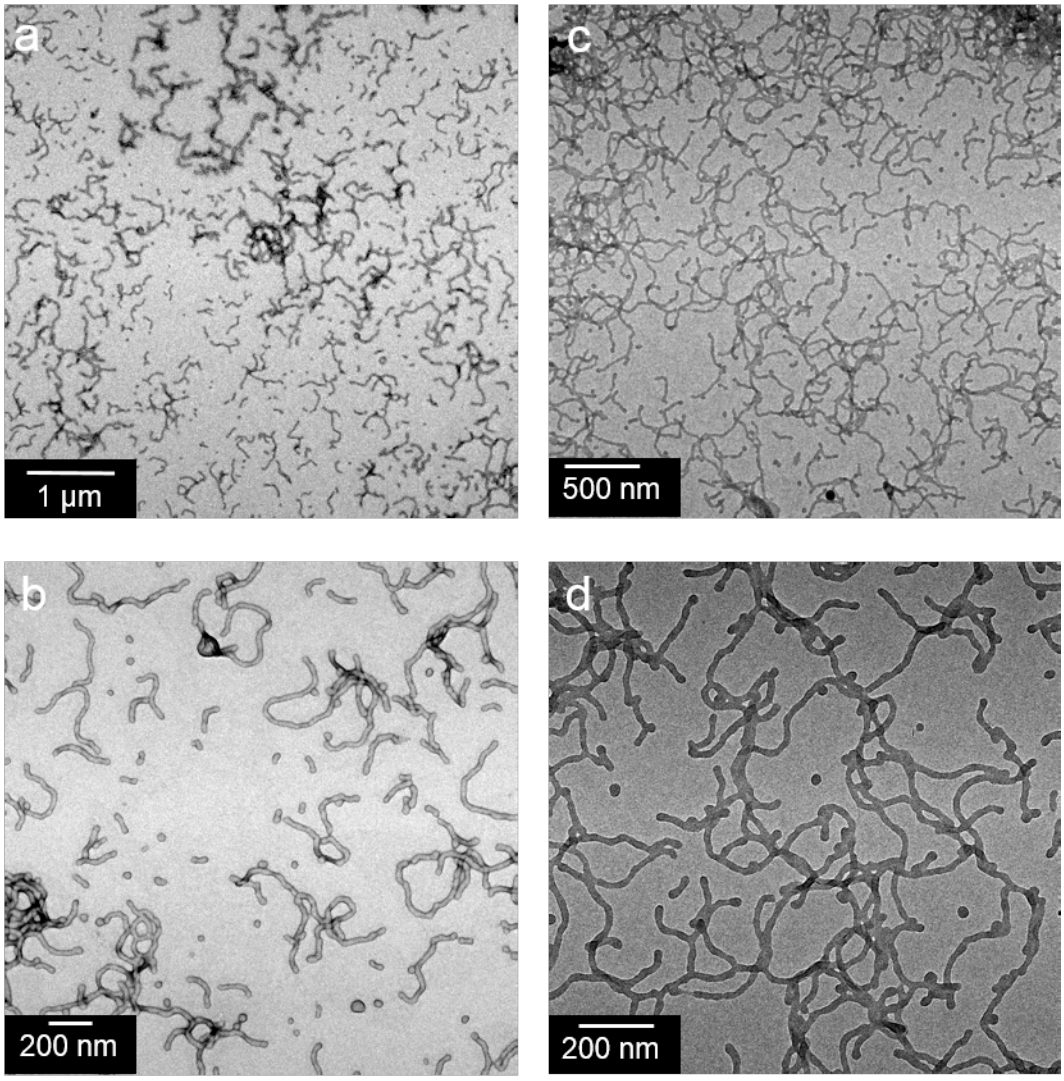

Figure S9. TEM of FMN, imaged 14 months after preparation.

a) and b) TEM of FMN, negative staining using 1% uranyl acetate

c) and d) TEM of FMN, no staining

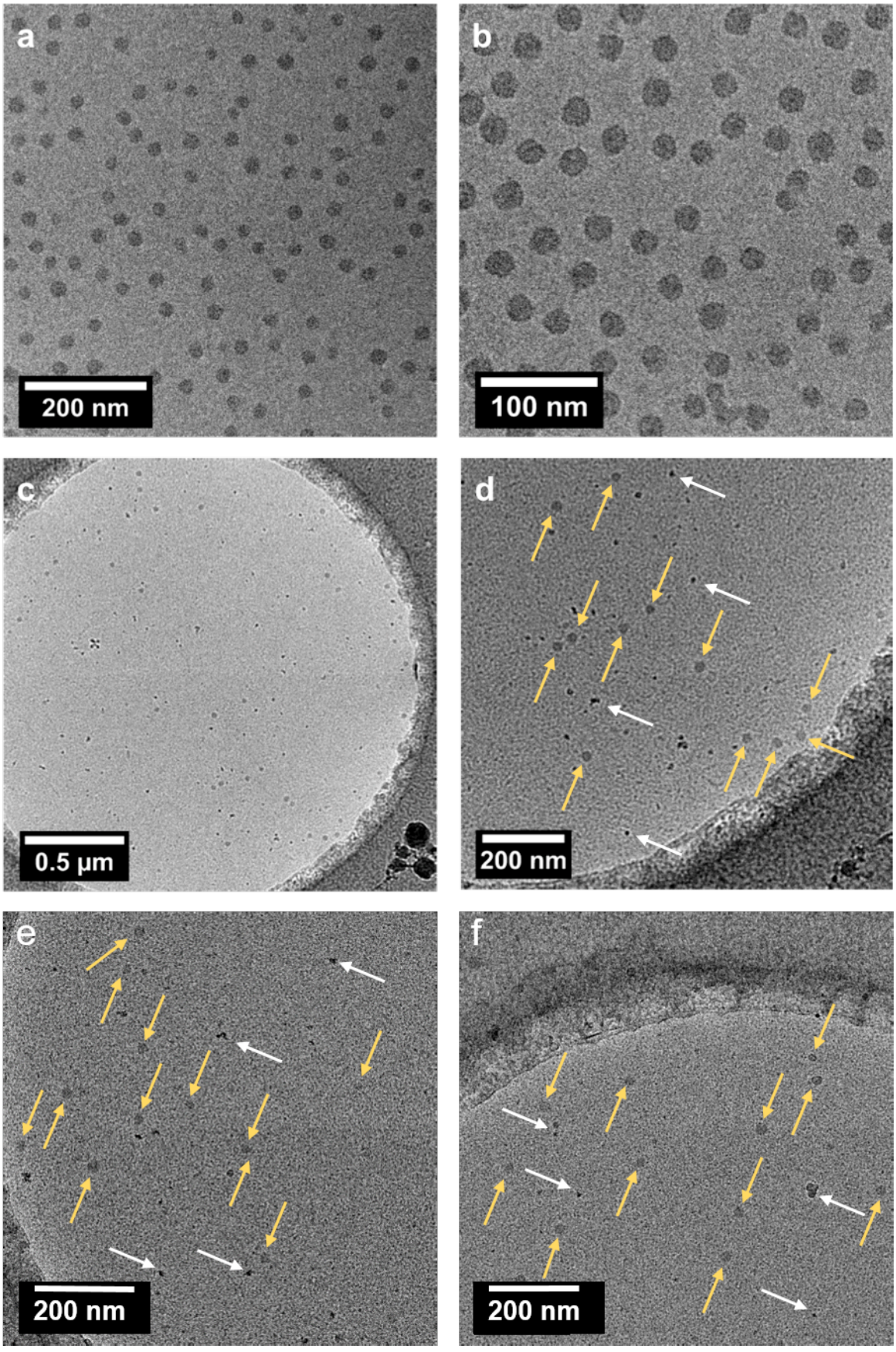
a
200 nm
b
100 nm
c
0.5 µm
d
200 nm
e
200 nm
f
200 nm

Figure S10. Stability of Nanomaterials in biological milieu: Cryo-TEM of SMN in Water and Blood Serum for 1 week

a) and b) Cryo-TEM of SMN in water.

c) - f) Cryo-TEM of SMN in blood serum after 1 week. 10 uL of SMNs in water was added to 10 uL of blood serum. Sample volume was reduced to 10 uL by evaporation under reduced pressure and stored at 37 ºC for 1 week prior to imaging. Yellow arrows in d, e and f indicate SMN, while white arrows indicate examples of ice artifacts stemming from cryo sample preparation.

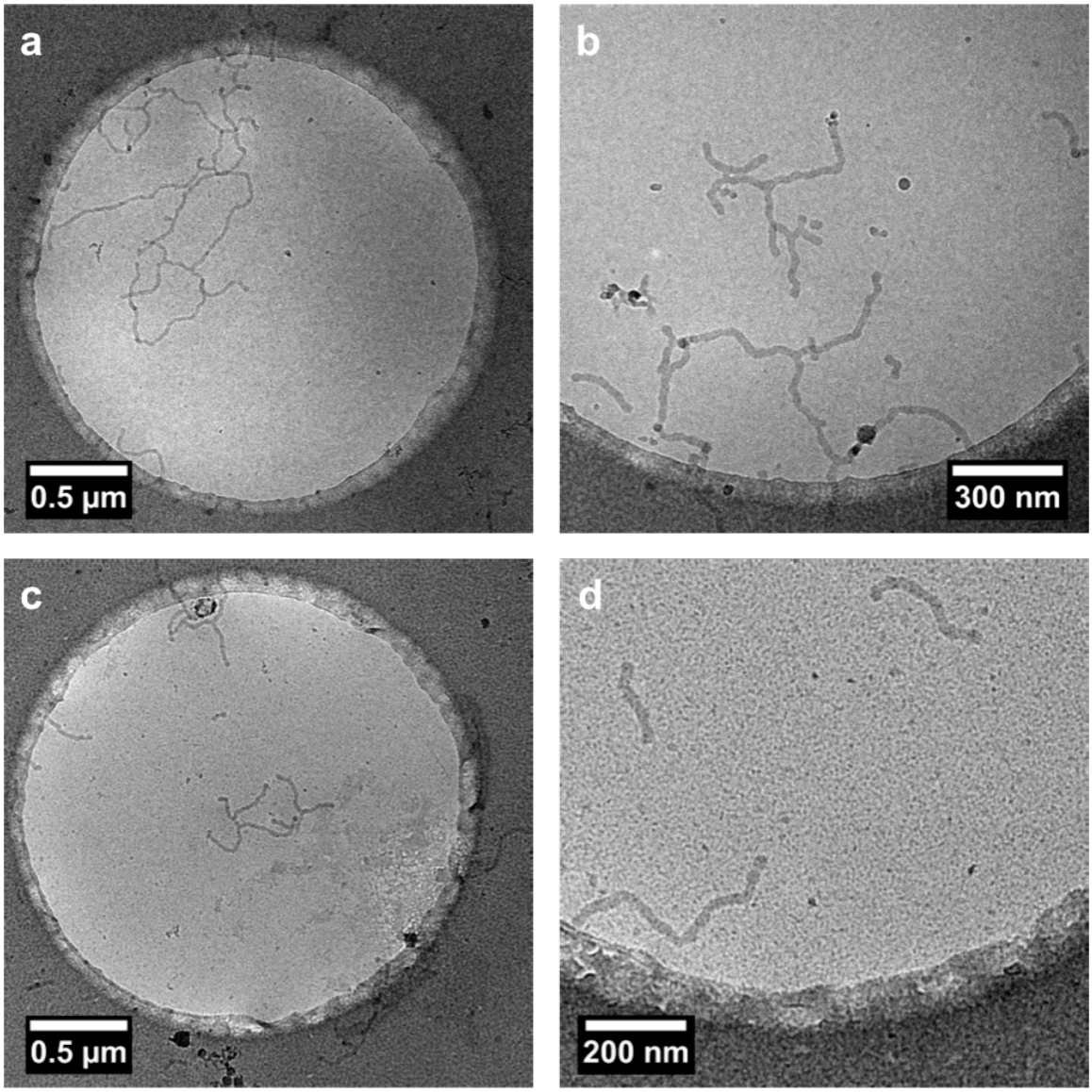

Figure S11. Stability of Nanomaterials in biological milieu: Cryo-TEM of FMN in Water and Blood Serum.

a) *and* ***b)*** *Cryo-TEM of* ***FMN*** *in water*

c) *and* ***d)*** *Cryo-TEM of* ***FMN*** *in blood serum. 10 uL of* ***FMN****s in water was added to 10 uL of blood serum The sample volume was reduced to 10 uL by evaporation under reduced pressure and stored at 37 ºC for 1 week prior to imaging.*

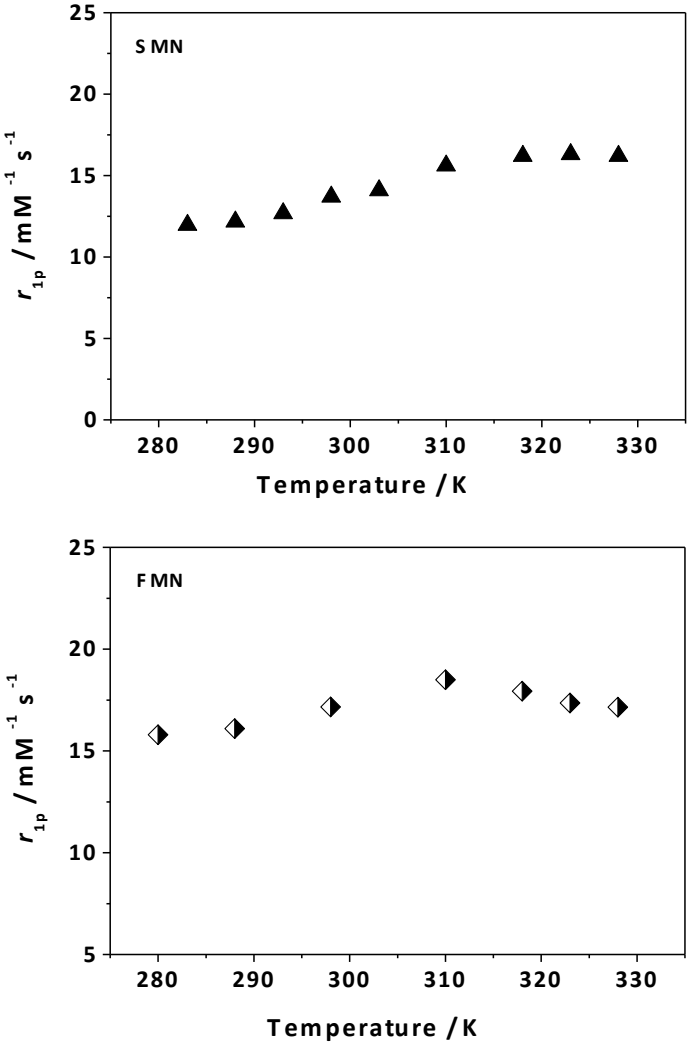

Figure S12 NMRD Proton relaxivity as a function of temperature for SMN and FMN at 20 MHz and pH=7.2 In the case of SMN (top) the relaxivity increases with temperature up to about 320 K and then it remains stable at higher temperatures. This behavior is associated with a longer value of the residence lifetime, which implies a more pronounced limiting effect on relaxivity. In the case of FMN the profile is characterized by a broad peak centered at about 305-315 K (bottom): this implies that around physiological temperatures relaxivity reaches a maximum value and it is not limited by the relatively slow exchange of the bound water molecule. A good fit of the NMRD data was obtained with $^{298}\tau_M$ values of 350 and 560 ns for FMN and SMN, respectively, in full agreement with the temperature-dependence study.

***In Vivo* MRI**

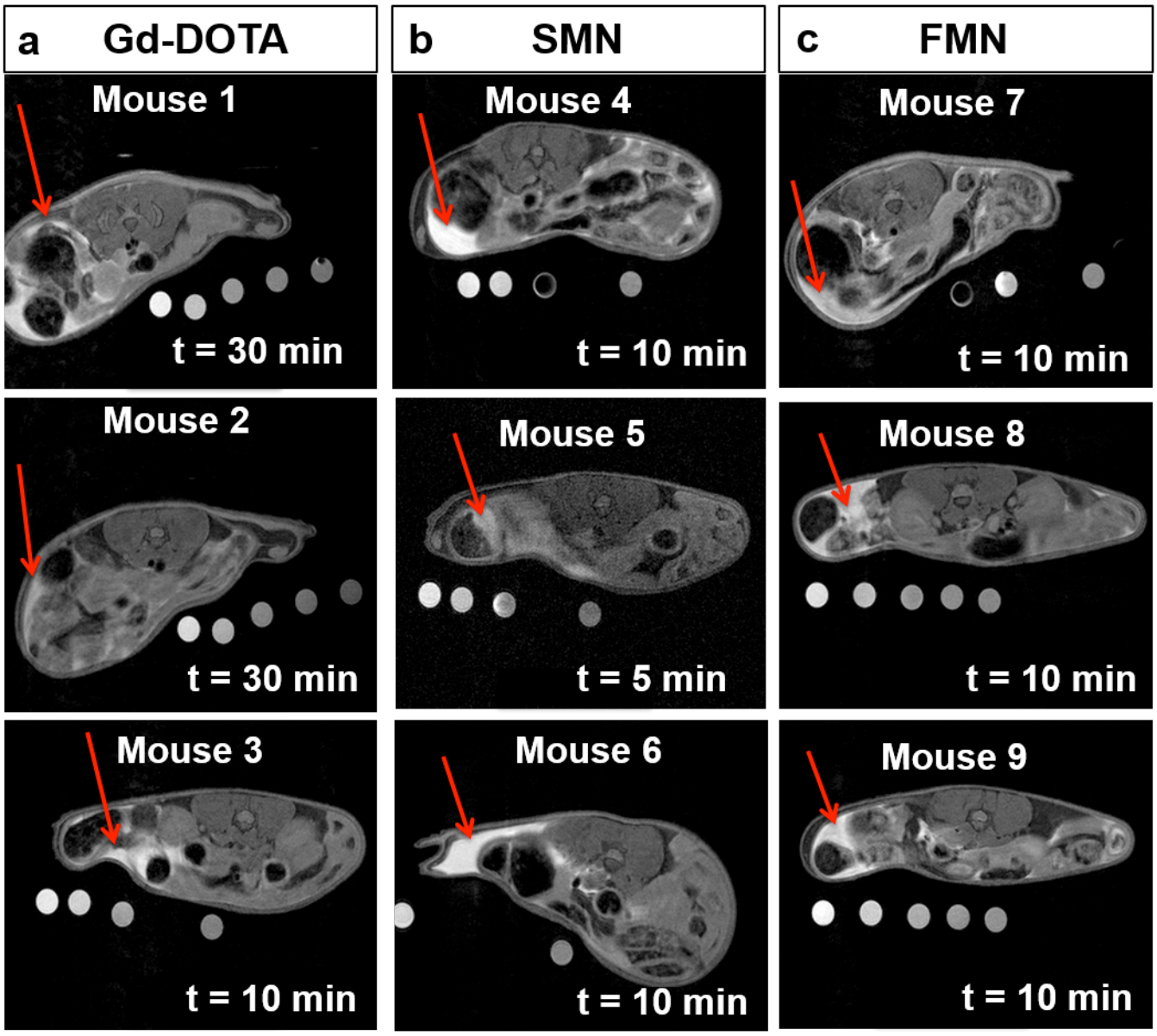

Figure S13. Anatomical MRI post-injection of contrast agent demonstrating successful introduction of materials IP. Red arrows indicate contrast surrounding the bowl loops.

a) *Anatomical image of mice 1 – 3, 10 – 30 minutes post-IP injection of Gd-DOTA.*

b) *Anatomical image of mice 4 – 6, 5 – 10 minutes post-IP injection of SMN.*

c) *Anatomical image of mice 7 – 9, 10 minutes post-IP injection of FMN.*

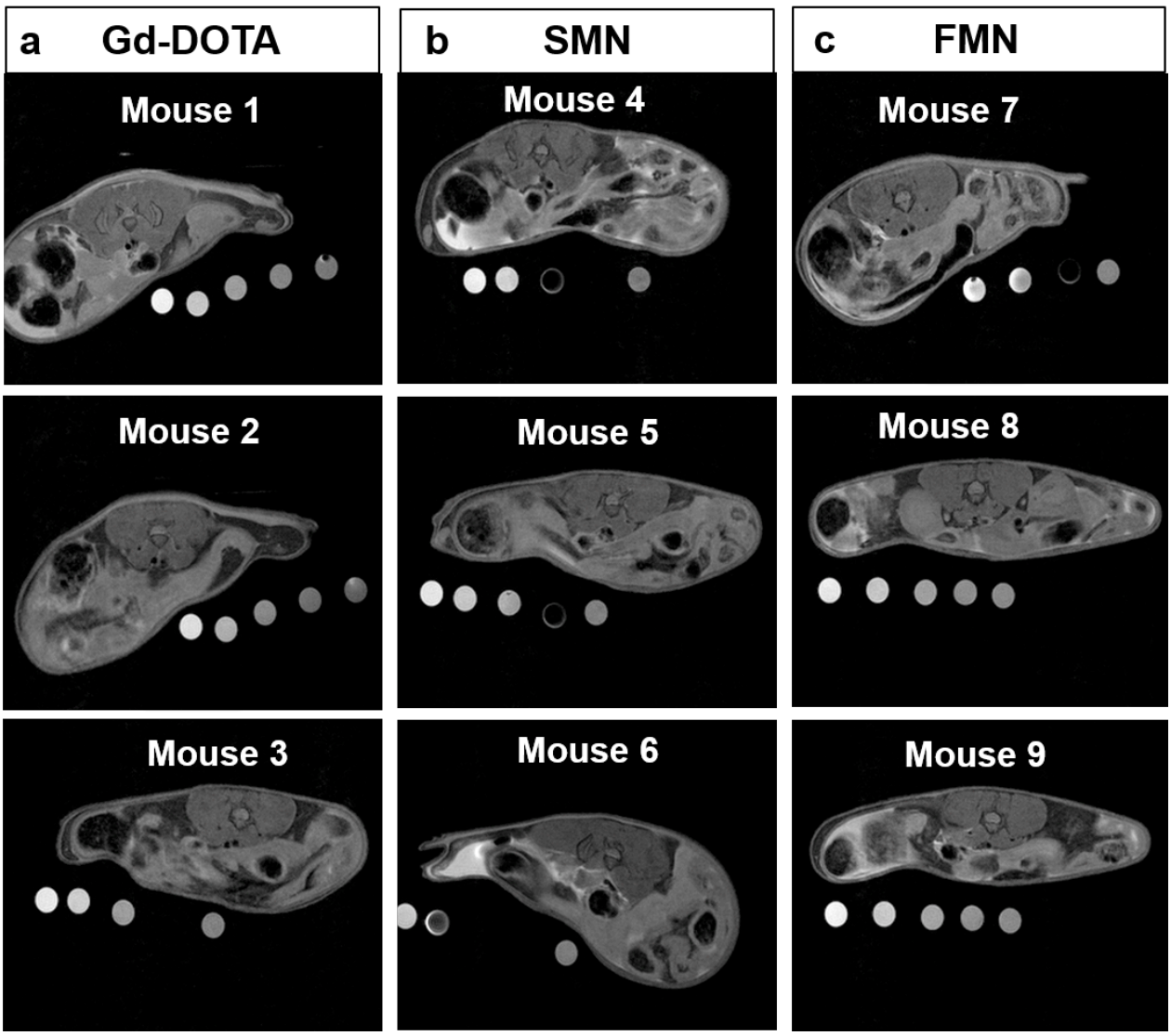

Figure S14. Anatomical MRI of IP space at two hours post-injection demonstrating no signal enhancement (for Gd-DOTA) or signal enhancement (for SMN and FMN): NP formulations are retained in the IP space longer than Gd-DOTA.

a) Anatomical image of mice 1 – 3, two hours post-IP injection of Gd-DOTA.

b) Anatomical image of mice 4 – 6, two hours post-IP injection of SMN.

c) Anatomical image of mice 7 – 9, two hours post-IP injection of FMN.

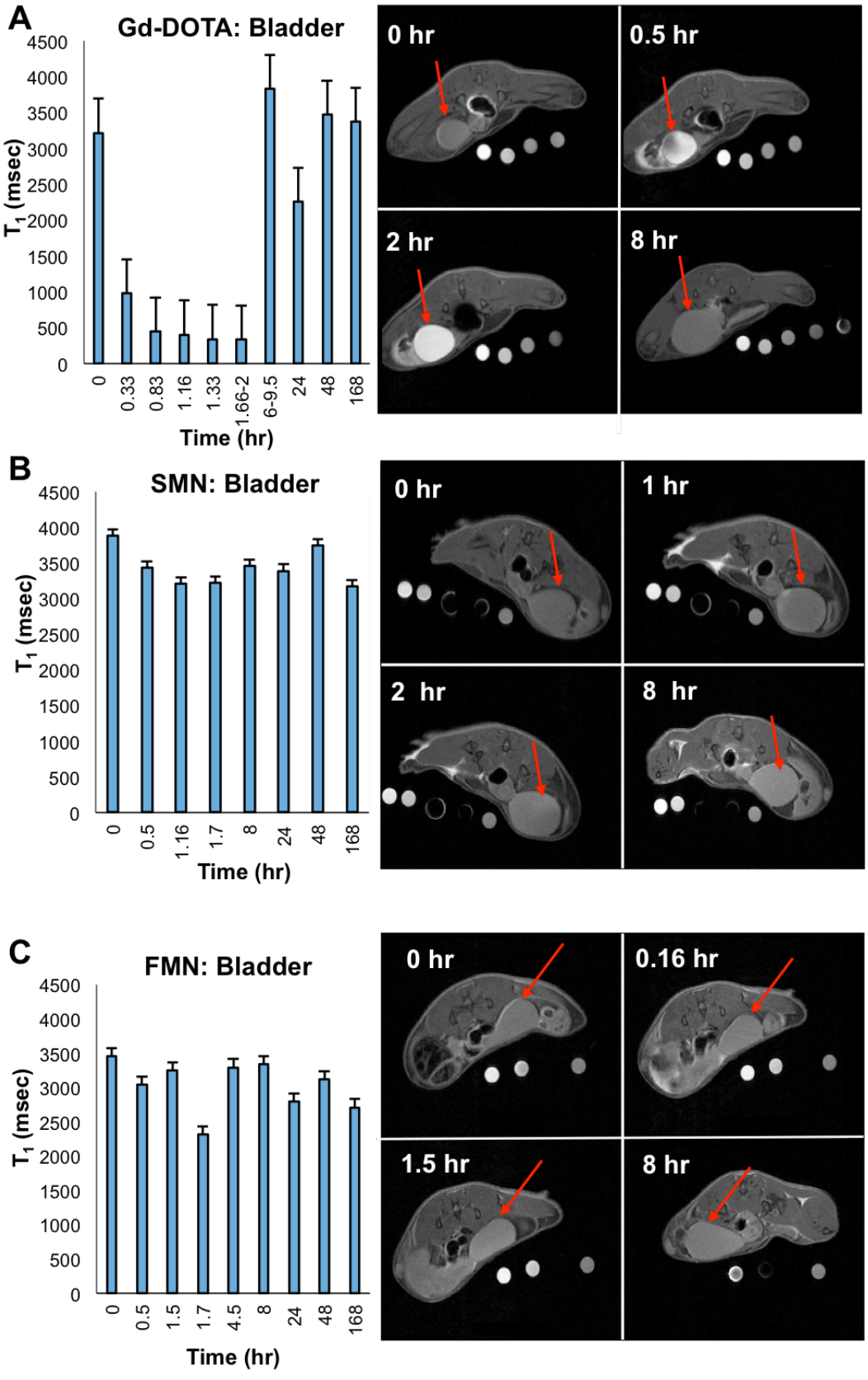
A
Gd-DOTA: Bladder
T1 (msec)
4500
4000
3500
3000
2500
2000
1500
1000
500
0
0
0.33
0.83
1.16
1.33
1.66-2
6-9.5
24
48
168
Time (hr)
0 hr
0.5 hr
2 hr
8 hr
B
SMN: Bladder
T1 (msec)
4500
4000
3500
3000
2500
2000
1500
1000
500
0
0
0.5
1.16
1.7
8
24
48
168
Time (hr)
0 hr
1 hr
2 hr
8 hr
C
FMN: Bladder
T1 (msec)
4500
4000
3500
3000
2500
2000
1500
1000
500
0
0
0.5
1.5
1.7
4.5
8
24
48
168
Time (hr)
0 hr
0.16 hr
1.5 hr
8 hr

Figure S15. Time progression of signal enhancement, quantified as T_1, and corresponding axial T_1-weighted images of the bladder after IP-injection of a) Gd-DOTA, b) SMN, and c) FMN. For mice 1-9, multiple regions of interest were sampled, normalized by comparing the relaxivity of phantoms for each scan to the pre-injection phantom relaxivity, averaged over the organ in the scan, then converted to T_1. For sampled time points of each material, T_1 times were averaged, and standard error generated for n = 3 mice. Red arrows indicate the urinary bladder.

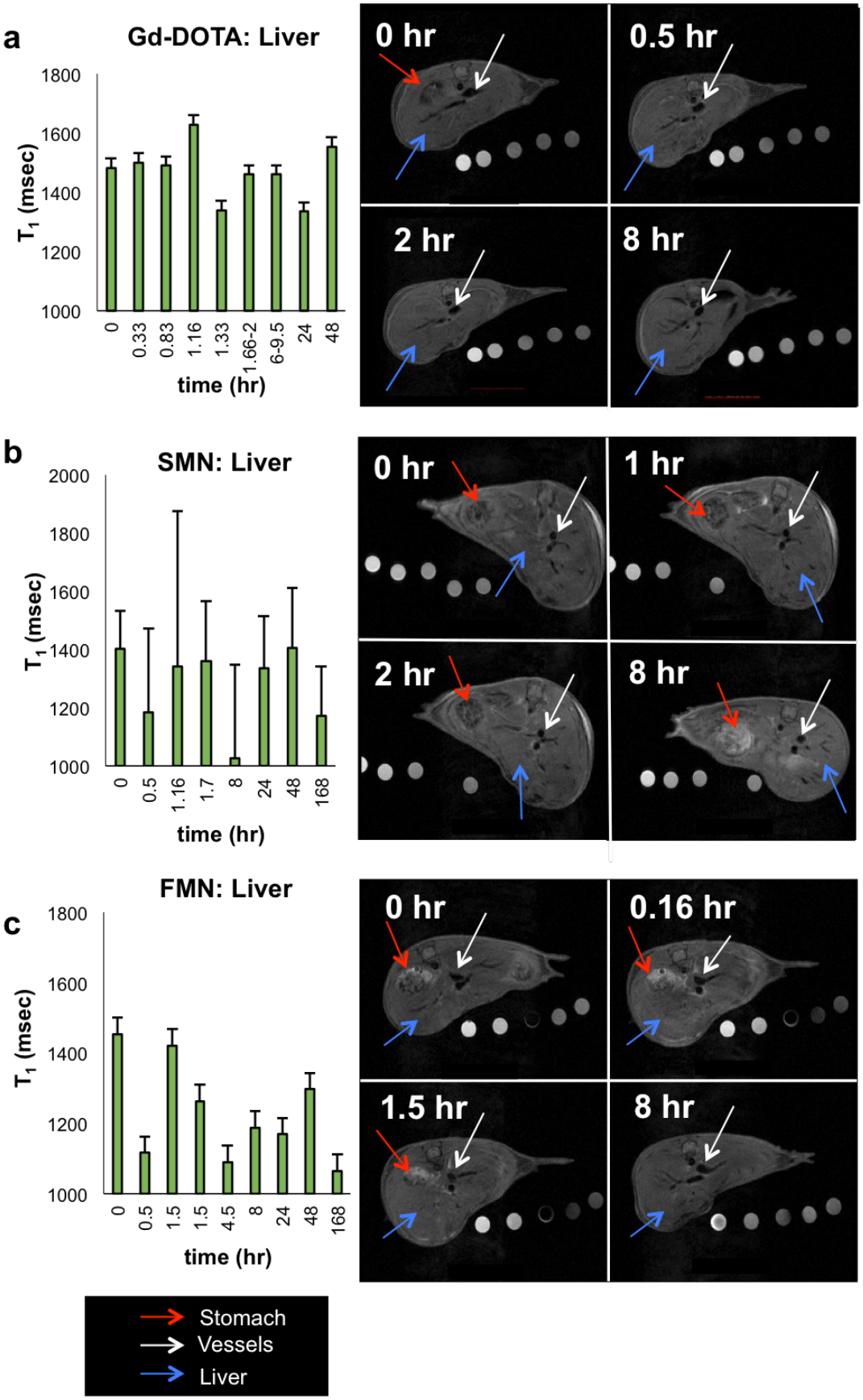
a
Gd-DOTA: Liver
T1 (msec)
1800
1600
1400
1200
1000
0
0.33
0.83
1.16
1.33
1.66-2
6-9.5
24
48
time (hr)
0 hr
0.5 hr
2 hr
8 hr
b
SMN: Liver
T1 (msec)
2000
1800
1600
1400
1200
1000
0
0.5
1.16
1.7
8
24
48
168
time (hr)
0 hr
1 hr
2 hr
8 hr
c
FMN: Liver
T1 (msec)
1800
1600
1400
1200
1000
0
0.5
1.5
1.5
4.5
8
24
48
168
time (hr)
0 hr
0.16 hr
1.5 hr
8 hr
Stomach
Vessels
Liver

Figure S16. Time progression of contrast enhancement, reported as T_1, and corresponding anatomical scans of the liver after IP-injection of a) Gd-DOTA, b) SMN, and c) FMN. Any contrast enhancement in the stomach is due to food, not injected material. Red arrows indicate the stomach, white arrows indicate a vessel, and blue arrows indicate part of the liver.

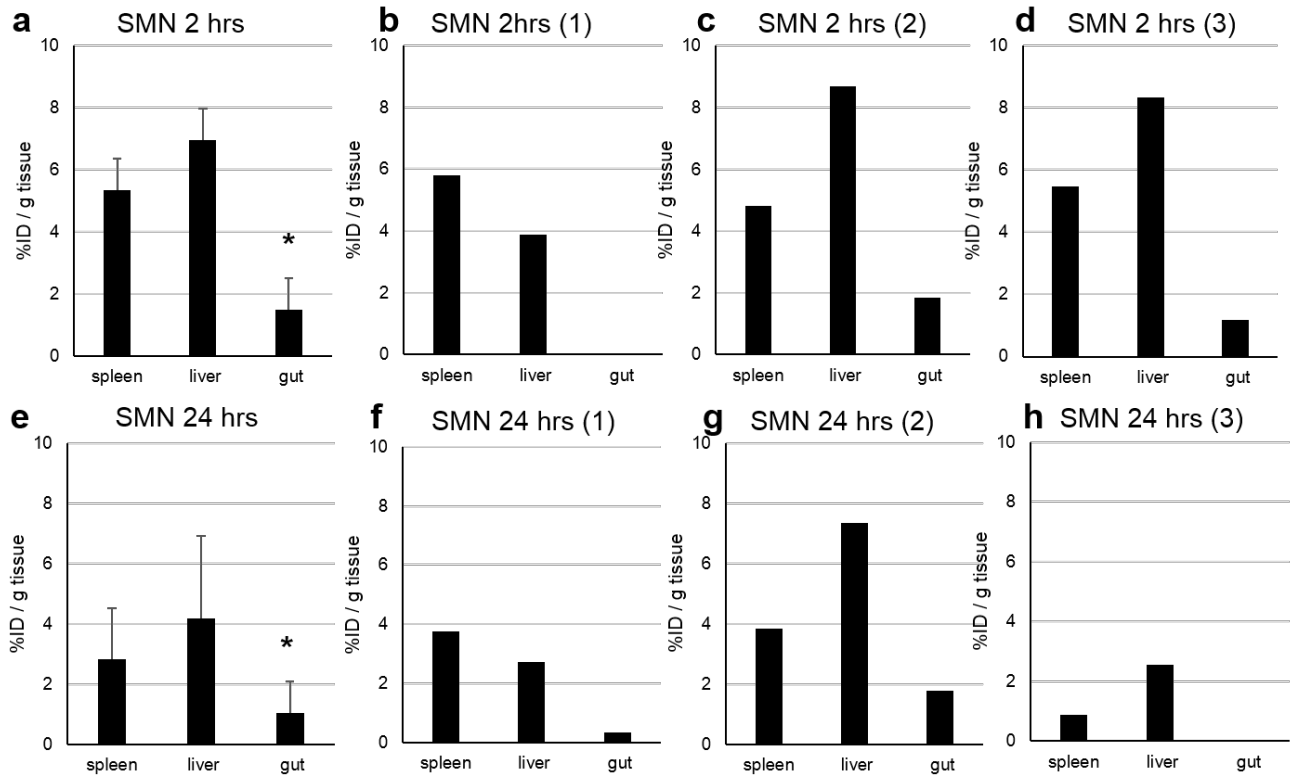

Figure S17 Average and three individual mice for SMN at 2 and 24 hrs. Graphs a and e are the average of three mice. Graphs b,- d, are individual mice sacrificed at 2 hours post injection. Graphs f - h are individual mice sacrificed at 24 hrs. Error bars are for n= 3 mice except where annotated with *, where n = 2.

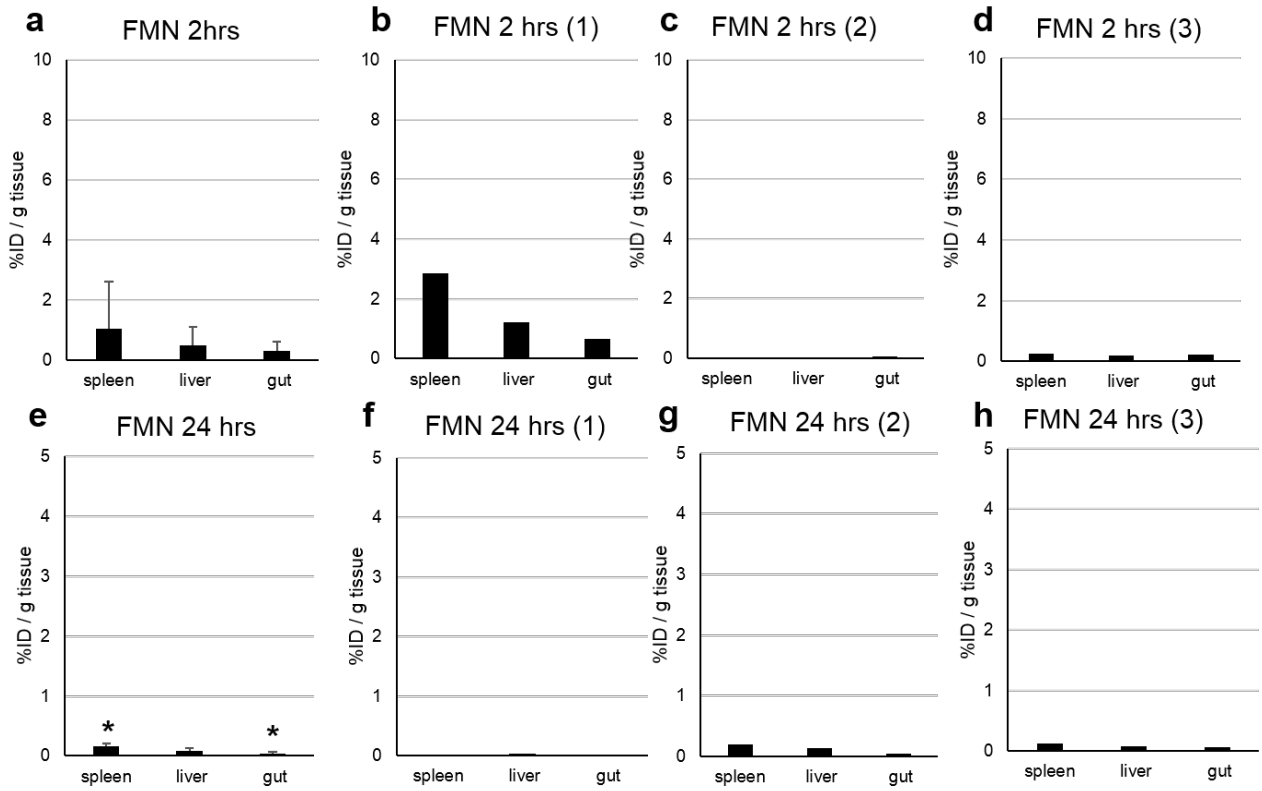

Figure S18. Average and three individual mice for FMN at 2 and 24 hrs. Graphs a and e are the average of three mice. Graphs b,- d, are individual mice sacrificed at 2 hours post injection. Graphs f- h are individual mice sacrificed at 24 hrs. Error bars are for n= 3 mice except where annotated with *, where n = 2.